



Contents lists available at ScienceDirect

CIRP Annals - Manufacturing Technology

journal homepage: <http://ees.elsevier.com/cirp/default.asp>

Mechanisms and processing limits of surface finish using laser-thermochemical polishing

Sandro Eckert^{a,*}, Frank Vollertsen (1)^{a,b}^aBIAS-Bremer Institute for Applied Beam Technology, Klagenfurter Str. 5, 28359 Bremen, Germany^bUniversity of Bremen, Klagenfurter Str. 2, 28359 Bremen, Germany

ARTICLE INFO

Keywords:

Laser
Polishing
Microstructure

ABSTRACT

Laser thermochemical machining allows a controlled material removal of metallic workpieces for an aesthetic or functionalized structuring. This work deals with the question, why does a smoothing effect occurs and what are the mechanisms behind it? The results show, that the surface smoothing is based on the preferred material removal of the roughness peaks compared to the valleys, as well as microstructure related limits of the surface quality. This might be caused not by one single, but a combination of electrical, thermal and physicochemical mechanisms. These effects can be used for the controlled and selective surface polishing.

© 2018 Published by Elsevier Ltd on behalf of CIRP.

1. Introduction

The ongoing trend of geometric complex parts with specific functionalized surface properties, often inspired by bionic concepts, pushes the need of more versatile and flexible manufacturing technologies. Due to its precise and flexible energy deposition laser based material processes are of increasing importance and often enable unique surface structures and properties. Especially, micromechanical parts used e.g. in biomedical applications have a high demand on function-oriented surface quality. Therefore, the parts require a machining without significant thermal impacts [1].

Short-pulsed lasers used in industry, often produce a noticeable heating of the material with solidified ablation debris and recast layer, which makes an electrochemical post-processing necessary. A direct and selective material processing with a high surface quality and gentle material removal can be accomplished by the laser induced thermochemical machining (LCM) [2].

Thereby, the laser radiation locally heats up the surface in an electrolyte ambient and enhances a chemical reaction by orders of magnitude [3]. The material removal mechanism is based on the laser induced thermochemical reaction between the electrolyte and metal atoms at the workpiece surface and can be deployed on all metals with a specific passivation layer. Due to the interaction between the laser radiation, workpiece material and liquid etchant, the local material removal and resulting surface quality is highly sensitive to the applied process parameters. Nevertheless, within a certain range of process parameters, disturbing influences on the surface quality caused by boiling electrolyte [4], metallic salt deposition or high temperature corrosion [5] can be avoided. In

this parameter window the laser thermochemical material removal can be used as a polishing process. On titanium a surface roughness of 0.1 μm can be achieved independent of the initial roughness [6].

In contrast to that, this paper shows that the extension of previous results to other microstructure and material systems is quite challenging, due to a lack of knowledge of the various influences on the polishing mechanism. To close this gap, the gradual surface evolution from the initial to the smoothed topography is investigated within repetitive processing steps. By this method, the chemical attack on the roughness is compared between the surface peaks and valleys.

2. Experimental

2.1. Laser thermochemical polishing setup

For a flexible and selective use of the laser thermochemical material removal as a surface polishing process a scanner based setup is used (Fig. 1). Thereby, it is important to ensure a controllable and disturbance-free laser energy deposition on the workpiece, considering the propagation throughout the liquid etchant environment. Therefore, the workpiece is mounted in an etching chamber, in which a 5 molar (28.7% vol.) phosphoric acid (H_3PO_4) is pumped as a cross-jet through a (25×2) mm^2 cross-section with velocity v_f of 2 m/s. On the one hand this provides a sufficient electrolyte support. On the other hand it ensures a fast evacuation of the emerging process gases out of the focus area. As laser source the fibre laser JK400 is used. Its TEM_{00} cw laser radiation of 1080 nm is focused by a telocentric f-theta optic and guided along the surface with 2 mm/s using the scanning system Raylase Superscan III-15. Using a telescope, the laser beam diameter and thus the focal spot diameter d is set to a value of 110 μm , which corresponds to an area A_0 of 9500 μm^2 .

* Corresponding author.

E-mail address: eckert@bias.de (S. Eckert).

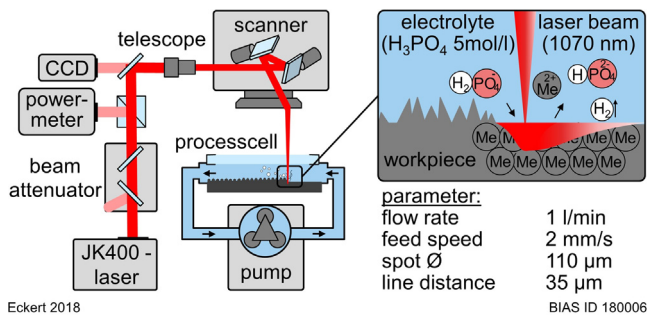


Fig. 1. Schematic illustration of the scanner based setup for the selective laser processing in a wet-etching environment.

2.2. Methodology and samples

In this study, two different parameter setups were chosen. On the one hand, (to investigate the temporal evolution) a titanium grade 1 sample was structured with parallel lines hatched with a distance of $35\ \mu\text{m}$ with a constant laser power of $3.1\ \text{W}$ to an array of $1\ \text{mm} \times 1\ \text{mm}$. This process was repeated between $N=5$ up to $N=3700$ times (Table 1a). While on the other hand, (to examine the influence of the microstructure) arrays with the same dimensions but each at a different laser power between $P=1.5\ \text{W}$ up to $P=5.5\ \text{W}$ were structured on differently manufactured stellite 21 samples. The number of repetitions per array was kept constant to $N=50$ (Table 1b). Prior to laser processing, all samples were sand blasted for $5\ \text{s}$ to set a defined initial roughness of $(2.2 \pm 0.2)\ \mu\text{m}$. All structured surfaces were characterized topographically by using the confocal laser-scanning microscope Keyence VK-9710.

Table 1

Overview of the varied process parameter and samples.

Section	Parameter	Label – Material/Sample
(a)-3.1	$N=5-3700$ $P=3.1\ \text{W}$	T1 – Titanium Grade 1
(b)-3.2	$N=50$ $P=1.5-5.5\ \text{W}$	S1 – spray formed S2 – cast S3 – additive manufactured (annealed $10\ \text{h}/1100^\circ\text{C}$) S4 – additive manufactured S5 – laser sintered

Microscope measurements were made after every repetitive scanning step for the titanium sample T1. For that, 5×4 (each covering a size of $1.3\ \text{mm} \times 0.8\ \text{mm}$) microscope images ($50\times$ objective) were assembled. All these height profiles were put above each other and adjusted by taking features of the unmodified surface as reference. This positioning adjustment is automated using Matlab routines. Due to better comprehensibility the number of repetitions N is converted to the effective laser radiation time per area unit $t_r = A_{\theta}/(b \cdot v) \cdot N$. Thereby, changes of individual surface features as well as statistic values like the S_a can be analyzed with respect to their time dependence.

In contrast to that, 2×2 microscope images were assembled (each covering a size of $0.5 \times 0.4\ \text{mm}$) for every array on the stellite 21 samples S1–S5. The surface roughness S_a was calculated with Matlab after applying a SL-filter in accordance to ISO 25178. Nevertheless, the roughness S_a is often insufficient for a quantitative evaluation of the machined surface, due to the lack of information about the height profile. For a further process development and parameter optimization of the laser-thermochemical polishing process, an analysis of the roughness for different spatial frequency wavelengths of the height profile was calculated. Therefore the Fourier transformation of the profile was bandpass filtered for cut-off intervals of $0-1.25-2.5-5-10-20-40-80-160-320\ \mu\text{m}$. Afterwards, the filtered spatial frequency spectra were transformed back to topographical images and their roughness $S_{a\lambda}$ calculated. The differentiated analysis of the roughness in micro- ($0.8-10\ \mu\text{m}$),

meso- ($10-80\ \mu\text{m}$) roughness and waviness ($80-320\ \mu\text{m}$) allows to visualize the impact of the machining process on multi-scale surface features.

3. Results

3.1. Smoothing mechanism

The gradual surface evolution of titanium was investigated by increasing the repetition steps, while all other processing parameters, like the laser power, hatching distance and scan velocity were kept constant. In contrast to previous works, the same surface section was investigated repeatedly. This enables a time-resolved microscopic study of the surface topography evolution.

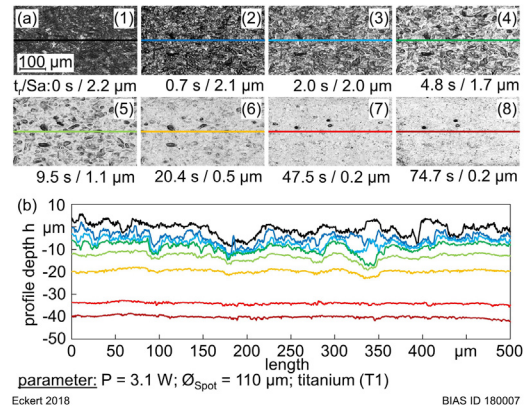


Fig. 2. (a) Microscope images and surface roughness of the sand blasted surface for different radiation times t_r and (b) the corresponding cross-section profile depth.

Fig. 2a1–8 shows the microscopic images of the surface finish for increased processing times from $0.7\ \text{s}$ to $74.7\ \text{s}$. The corresponding surface profile with respect to the measured depth are shown colour-coded in Fig. 2b. The picture series starts with the sand blasted surface topography (Fig. 2a1) with a roughness S_a of $2.4\ \mu\text{m}$. With increasing process time, the smoothing of the surface becomes visible through the optical brightening of the images (Fig. 2a3). After $9.5\ \text{s}$ the surface (Fig. 2a5) is predominated by the surface valleys. These are surrounded by mainly plain surface areas. The roughness is already reduced to $1.1\ \mu\text{m}$. In the surface profiles (Fig. 2b) the time dependent evolution of the peaks and valley can be observed, too. With increasing time to $47.5\ \text{s}$ the surface is smoothed to a S_a of $0.2\ \mu\text{m}$ (Fig. 2b7). As seen in Fig. 2a8, an even further increase in processing time has no effect on the surface quality anymore. The surface topography is just lowered in depth (Fig. 2b, red) while the surface roughness of $0.2\ \mu\text{m}$ could not be improved anymore.

The surface depth of every particular time step, thus the material removal depth, is calculated by the two dimensional mean value for every surface topography. This mean removal depth is depicted by the black measurement points in Fig. 3 in a double logarithmic scale. For a more differentiated view, the surface topography is separated into surface peak and valley areas as shown in the legend in Fig. 3. The mean peak removal depth is defined by the 10 % of the highest (red) surface parts. Equally the mean valley removal depth is defined by the 10 % of the lowest (blue) surface parts. The initial difference between the mean peak removal depth and mean valleys depth amounts $13.5\ \mu\text{m}$. With increasing process time this difference decreases continuously to $1.3\ \mu\text{m}$ after $20\ \text{s}$. Further it is to be noticed, that in the first seconds from $0.7\ \text{s}$ to $2.1\ \text{s}$ the removal rate (gradient of mean removal depth) of the mean peak removal depth is more than 3.5 times higher than for the mean valley depth. After $20\ \text{s}$ the removal rate of the mean peak removal depth (Fig. 3, red) and valley (Fig. 3, blue) approached nearly the same value. After that time the distinction between peaks and valleys becomes obsolete.

Download English Version:

<https://daneshyari.com/en/article/8038711>

Download Persian Version:

<https://daneshyari.com/article/8038711>

[Daneshyari.com](https://daneshyari.com)